IMPERIAL COLLEGE LONDON

DEPARTMENT OF LIFE SCIENCE

???

Author:
Quqiming Duan

Supervisor:
Samraat Pawar

A thesis submitted for the partial fulfillment of the requirements for the degree of Master of Research at Imperial College London

June 27, 2021

Declaration

Contents

1 Abstract

2 Introduction

Microbes is the most diverse group of organisms known on Earth and plays a crucial role in biogeochemical cycling fundamental for a wide range of ecosystem functions.

The emergence and maintenance of microbial communities' structures under natural and anthropogenic environmental conditions remain central topics in the field of microbial ecology. Current research in dissecting the mechanisms of community assembly generally accept the simultaneous operation of deterministic and stochastic processes (Chase & Myers 2011, Posfai et al. 2017, Goyal et al. 2018, Tilman 2004), that the emergence of community structures is governed by fitness selection (survival and growth), drift, speciation and spatial dispersal (Vellend 2010). And these ecological processes are influenced by nutrient availability, environmental filtering (e.g. temperature, pH, moisture) and interspecies interactions (e.g. cross-feeding, competition) (Chesson 2000).

Temperature is one of the fundamental factors for microbial metabolism, regulating the reaction rates of enzyme activities which controls growth rate and species interactions. In response to the rapid development of sequencing technologies (Kirk et al. 2004, Theron & Cloete 2000, Tiedje et al. 1999), rising number of empirical field studies were conducted interpreting the diversity patterns of microbial communities, however have reported different results regarding the tendency of microbial diversity across temperatures (Thompson et al. 2017, Zhou et al. 2016, Kolton et al. 2019). The hardship in deriving a universal temperature response pattern for diversity is generally caused by the difficulty in disentangling multiple biotic and abiotic impacting factors in determining community structure (Zhou et al. 2020, Hendershot et al. 2017).

Microbial carbon use efficiency (CUE) reflects the ability of organics decomposition in relation to the ecosystem function of carbon cycling. CUE describes the ratio of carbon assimilation and carbon intake, which considers organic matter decomposition, biomass production and carbon loss through respiration and extracellular secretion of organic carbon (Bardgett et al. 2008). The general effect of temperature on CUE is difficult to predict since all processes mentioned above are related to microbial metabolism and enzyme reactions, which would all be impacted by temperature factor (Davidson & Janssens 2006, Gang 2019, Smith et al. 2019) but at different degrees depending on their temperature sensitivity.

While Domeignoz-Horta et al. (2020) reported the positive correlation between soil microbial diversity and CUE through an empirical study on global warming, the selection of CUE during the stabilizing process of the community can also be a driver for regulating community diversity.

This study aims at understanding the role environmental temperature plays on microbial diversity and CUE. In this study, I disentangle the natural abiotic deterministic factors impacting community assembly, focus on the emergence of heterotrophic mesophilic bacterial community diversity patterns under operational temperatures, the CUE patterns of the resultant communities, and the

relationship between microbial diversity and CUE.

I start with randomly generated microbial communities to circumvent the issue of the complication of numerous hard-to-measure parameters in ecosystems, with the idea that the general resource-consumer model with random parameters can reproduce empirical observations of microbial community assembly (Goldford et al. 2018). Then impose selective pressure of resources and interspecies interactions under thermodynamic constraints, using temperature responses of species traits derived from empirical data.

3 Methods

3.1 Biomass and resource dynamics model

The core model used in this study was first adapted by Tom Clegg and Dr. Emma Cavan from Consumer-Resource Models in MacArthur (1970) and Marsland III et al. (2019), then further adapted into the current version, considering the concentration dynamics of N species of heterotrophic mesophilic bacteria consumers competing for M types of resources.

The consumer (C) biomass concentration (g/mL) dynamic is modelled by calculating the carbon resource requirement for exponential growth: the gain of carbon through resource uptake, minus the loss of carbon through inefficiency during uptake and the transformation of compound (metabolic secretion and maintenance respiration). The resource (S) concentration (g/mL) dynamic is modelled by calculating carbon inflow minus outflow. The inflow of each resource includes a constant abiotic external supply, the leakage during consumers' uptake, and the metabolic by-products biochemically transformed from other resources; the outflow is the total uptake of the resource by all consumers.

The biomass concentration dynamic of species i:

$$dC_i/dt = C_i\Big(\sum_{j=1}^{M} U_{ij}s_j(1-\sum_{k=1}^{M} l_{jk}) - R_i\Big) \tag{1}$$

The resource concentration dynamic of resource j:

$$dS_j/dt = \rho_j - \sum_{i=1}^{N}\Big(C_iU_{ij}s_j - \sum_{k=1}^{M} C_iU_{ik}s_kl_{kj}\Big) \tag{2}$$

In these equations above, we are only considering a Type I functional response, assuming a linear relationship between resource consumption and growth rate. U_{ij} is the uptake preference of the M resources by species i. On species level, uptake U_i follows the temperature and size dependencies and is randomly assigned across M resources (Figure 1: left plot). l_{jk} follows the leakage-transformation matrix with total leakage summing up to 0.4 for each resource ($l_j = 0.4$), when $j = k$, l_{jk} value is the leakage fraction resulting from the inefficiency of the resource uptake; when $j < k$, l_{jk} value is the

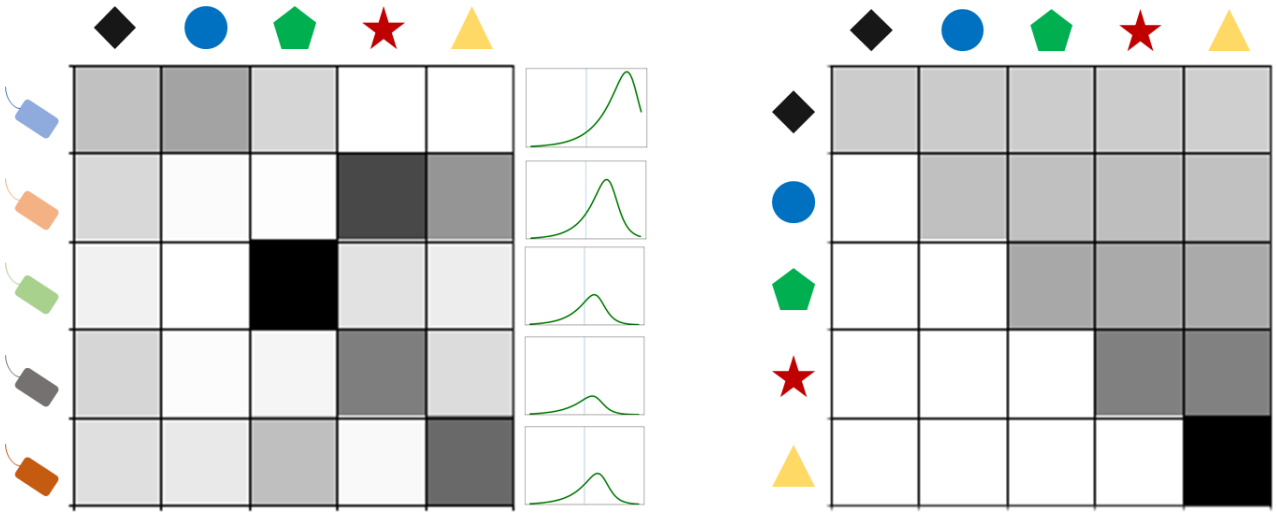

Figure 1: An example of random resource uptake distribution matrix (U_{ij}) of 5 species competing for 5 resources at 25 °C (left), darker color represents higher uptake rate of the consumer on certain resource. The line plots on the side presents the temperature dependence curve of uptake rate for each species (U_i), the vertical line in the middle of every plot dictates the value of uptake rate at 25 °C. An example of leakage-transformation matrix (l_{ij}) for 5 resources, with $l_j = 0.4$ (right). Darker color represents higher leakage/transformation of the resource from i to j.

biochemical transformation of resource j into k; when $j > k$, l_{jk} values are 0, for I am considering the reactions to be irreversible following the second law of thermodynamics (Figure 1: right plot). R_i is the carbon loss of species i through maintenance respiration. ρ_j is the concentration of abiotic external supply for resource j.

3.2 Temperature and size dependencies

The uptake and respiration rates in the model are considered size and temperature dependent following the Metabolic Theory of Ecology and a modified version of the Schoolfield equation (Kontopoulos et al. 2020), assuming both metabolic rates are controlled by single enzymes whose reaction rates are determined by temperature, and deactivate outside operational temperature range.

Temperature and size dependencies for resource uptake (U) and maintenance respiration (R):

$$U_{ij} = \frac{B_U m^{-1/4} \times e^{\frac{-Ea_U}{k} \cdot \left(\frac{1}{T} - \frac{1}{T_{ref}}\right)}}{1 + \frac{Ea_U}{E_{D_U} - Ea_U} e^{\frac{E_{D_U}}{k} \cdot \left(\frac{1}{T_{pk_U}} - \frac{1}{T}\right)}} \tag{3}$$

$$R_i = \frac{B_R m^{-1/4} \times e^{\frac{-Ea_R}{k} \cdot \left(\frac{1}{T} - \frac{1}{T_{ref}}\right)}}{1 + \frac{Ea_R}{E_{D_R} - Ea_R} e^{\frac{E_{D_R}}{k} \cdot \left(\frac{1}{T_{pk_R}} - \frac{1}{T}\right)}} \tag{4}$$

Note that the parameters values for these equations are given according to Smith et al. (2019), assuming that resource uptake rates have similar thermal sensitivity with bacterial growth rates (Figure 2). All temperature terms are in the unit of Kelvin(K).

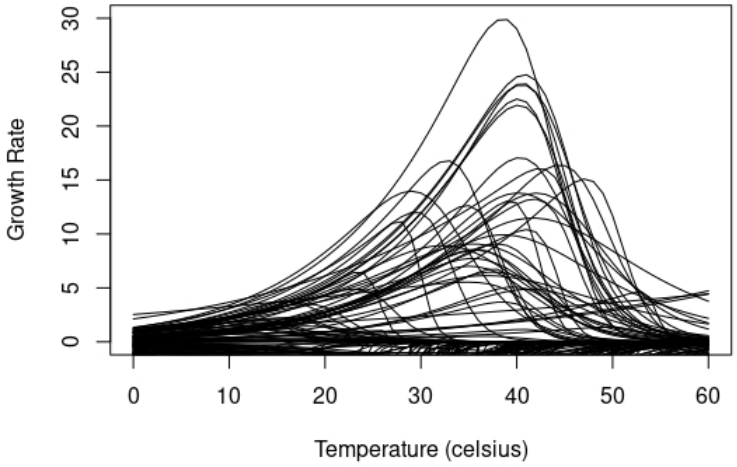

Figure 2: The temperature dependence curves of bacterial growth rates generated using a global data set collected and standardized in Smith et al. (2019).

In these equations, the metabolic rates are normalized to biomass specific for each consumer with $B = B_0 m^{(-\frac{1}{4})}$ where m is the biomass of the organism, and are all given a value of 1 g in this model since we are not discussing the size effects during assembly. Assuming both metabolic rates curves have the lowest variation at 0°C, I set B_U and B_R to be 2 (unit: 1/time) and 1 (unit: g/mL) at reference temperature (T_{ref} = 0). k is the Boltsmann constant, $8.617 \times 10^{-5} eVK^{-1}$. T is the simulation temperature under which the model is run. T_{pk} is the temperature for highest metabolic rates and also is the deactivation temperature for related enzyme, T_{pk} for uptake is sampled from a normal distribution with mean value at 308.15 K, and 3 degrees higher for respiration. E_a values are the activation energies, sampled from beta distributions with median values of 0.82 ev and 0.67 ev for uptake and respiration. E_D values are the deactivation energies, set to 3.5 eV for all reactions. U_0 and R_0 are the uptake and respiration rates at reference temperature.

Figure 3 demonstrates an example of randomly generated temperature dependent uptake and respiration curves of 100 species.

3.3 Simulation and species richness

The simulation for community assemblies is run on Python.

For each assembly, I start the system with a random pool of 100 species competing for 50 resources. The initial biomass concentration for each species is 0.1 g/mL and the initial resource concentration for each resource is 1 g/mL. Then run the selection process by integrating the concentration dynamics differential equation of species and resources (equation 1 & 2), as demonstrated in the upper figures of Figure 9. The running time is set to 4000 for all systems to reach steady state ($dC_i/dt = 0$ and $dS_j/dt = 0$), with a constant flux of externally supply of resource at each time point

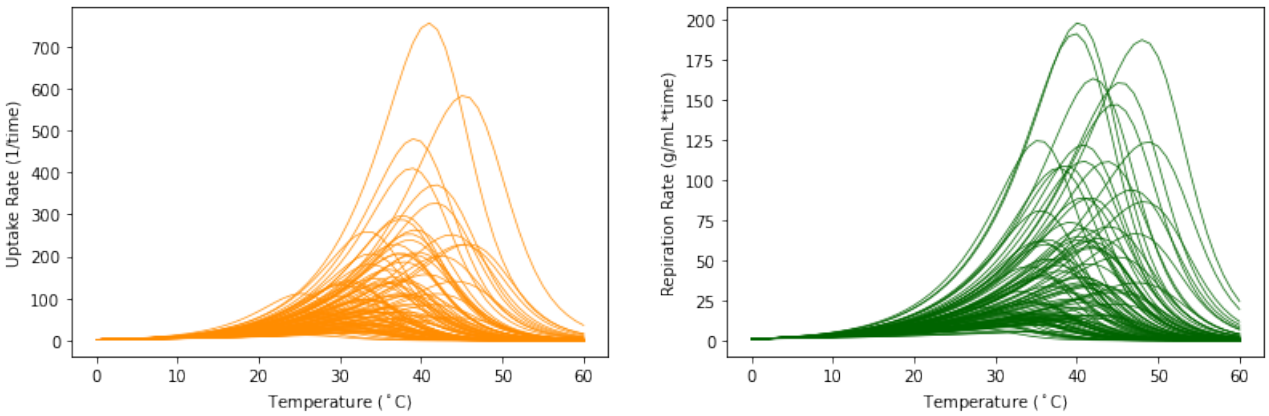

Figure 3: The temperature performance curves of uptake (left) and respiration (right) rates of 100 species. The activation energies are randomly sampled from beta distributions with median values of 0.82 eV and 0.67 eV, peak temperatures are randomly sampled from normal distribution with mean values of 308.15 K and plus 3 degrees for respiration.

($\rho_j = 1$).

Then the consumer and resource concentrations are returned to initial values and the next assembly is run with regenerated set of random species, as shown in the lower figures of Figure 9. This system simulates 30 parallel assemblies at each temperature, for all temperatures inside species' operational temperature range (0 - 25 °C).

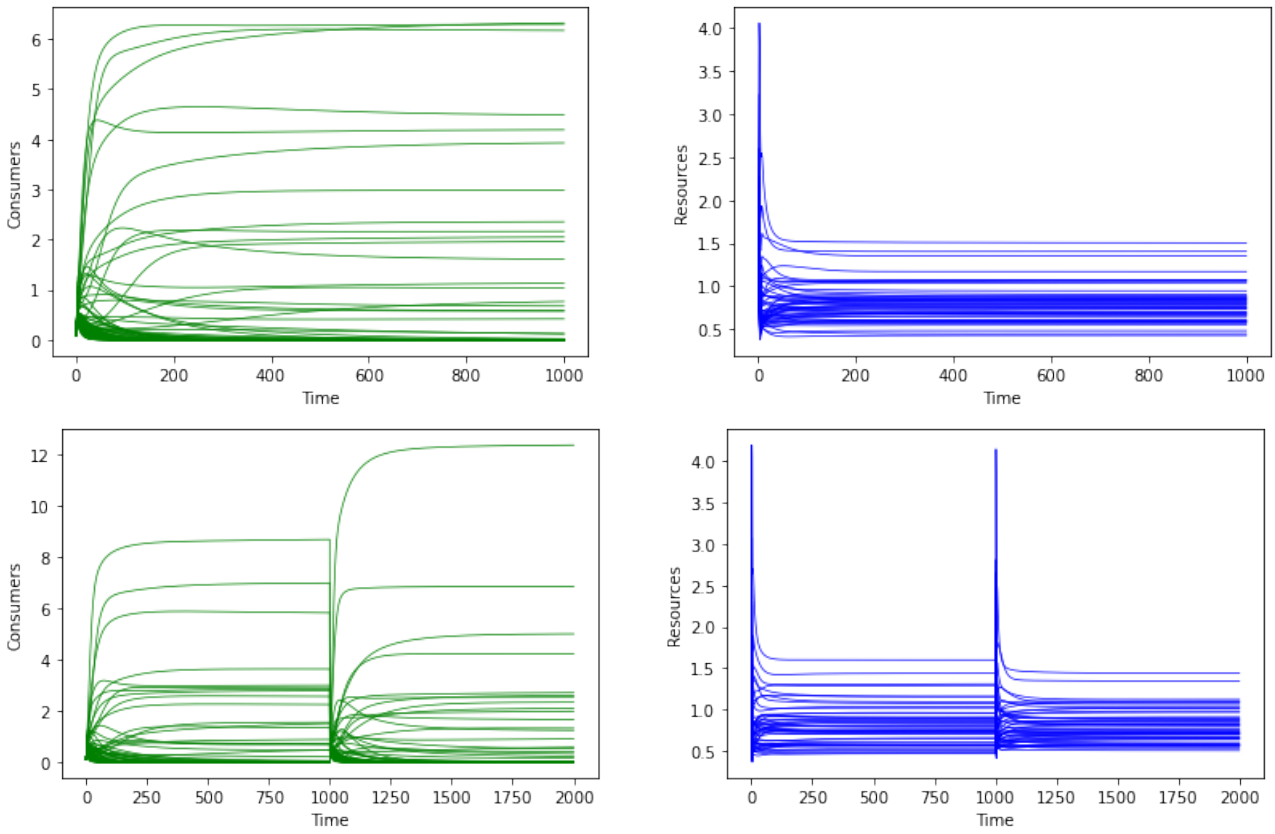

Figure 4: Example plots showing the consumer biomass and resource concentration dynamics of one assembly (upper two plots), and two parallel assemblies on continuous time (lower two plots.)

The species richness values are counted at steady state at the end of each assembly, as the number of species with positive biomass concentration ($C_i > 0$). The species richness of the communities decay as the systems reach steady states (Figure 5).

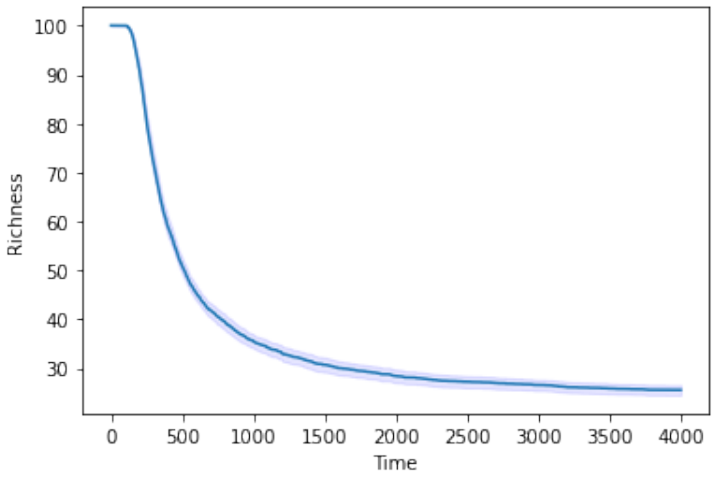

Figure 5: Example plot showing the average diversity decay during community stablizing of 30 parallel assemblies (CI = 0.95) at reference temperature (T = 0).

3.4 Calculation for CUE

We consider CUE as an intrinsic value for each species, encoded in the species' preference for uptake, leakage and transformation ability of carbon source, and maintenance respiration required for survival. These CUE values are then selected during assembly.

The intrinsic CUE value of species i is calculated with a common CUE calculation method using $\frac{\text{Carbon Gain}-\text{Carbon Loss}}{\text{Carbon Gain}}$ (Manzoni et al. 2012)

$$CUE_i = \frac{\sum_{j=1}^{M} U_{ij} s_{j0} (1 - \sum_{k=1}^{M} l_{jk})}{\sum_{j=1}^{M} U_{ij} s_{j0} + R_i} \tag{5}$$

S_0 here is the initial resource concentration at the beginning of the assembly, which is 1 g/mL.

According to Smith et al. (2020), the temperature response of CUE for organisms within the operational temperature range (OTR) has the form of the Boltzmann-Arrhenius equation. Here I give a similar calculation process of the intrinsic CUE based on equation 5, assuming the exponential increase of metabolic rates with temperature is equivalent to the Boltzmann-Arrhenius equation.

$$CUE = \frac{U_0 e^{\frac{-Ea_U}{k} \cdot \left(\frac{1}{T} - \frac{1}{T_{ref}}\right)} (1 - l) - R_0 e^{\frac{-Ea_R}{k} \cdot \left(\frac{1}{T} - \frac{1}{T_{ref}}\right)}}{U_0 e^{\frac{-Ea_U}{k} \cdot \left(\frac{1}{T} - \frac{1}{T_{ref}}\right)}} \tag{6}$$

The species CUE value at reference temperature ($T = T_{ref}$):

$$CUE_0 = \frac{U_0(1-l) - R_0}{U_0} \tag{7}$$

If we take a log form of equation(6), and assign $\Delta T = \frac{1}{k}\left(\frac{1}{T} - \frac{1}{T_{ref}}\right) \to 0$, then we can calculate the approximation of CUE as the first-order Taylor expression:

$$\begin{aligned} lnCUE &= ln(U(1-l) - R) - lnU \\ &\approx ln(U_0(1-l) - R_0) - lnU_0 + (\frac{R_0E_R - R_0E_U}{U_0(1-l) - R_0})\Delta T \end{aligned} \tag{8}$$

Which equation has the form of an Arrhenius equation, so if we take CUE_0 out of the equation, we can see the activation energy of CUE as:

$$Ea_{CUE} = \frac{R_0(E_U - E_R)}{U_0(1-l) - R_0} \tag{9}$$

3.5 Interspecies Interaction

The interspecies interactions (competition and cross-feeding) matrices are calculated using the weighted Jaccard similarity coefficient.

The competition index (J_c) for resources between species α and β is represented by the overlaps of resource uptake values:

$$J_c = \frac{\sum_{j=1}^{M} min(U_{\alpha j}, U_{\beta j})}{\sum_{j=1}^{M} max(U_{\alpha j}, U_{\beta j})} \tag{10}$$

The cross-feeding index (J_f) of resource j from species α to β is calculated with the overlaps of the biochemical transformation of all resources to resource j by species α and the uptake value of resource j by species β:

$$J_f = \frac{\sum_{j=1}^{M} min(\sum_{k=1}^{M} U_{\alpha k} l_{kj}, U_{\beta j})}{\sum_{j=1}^{M} max(\sum_{k=1}^{M} U_{\alpha k} l_{kj}, U_{\beta j})} \tag{11}$$

4 Results

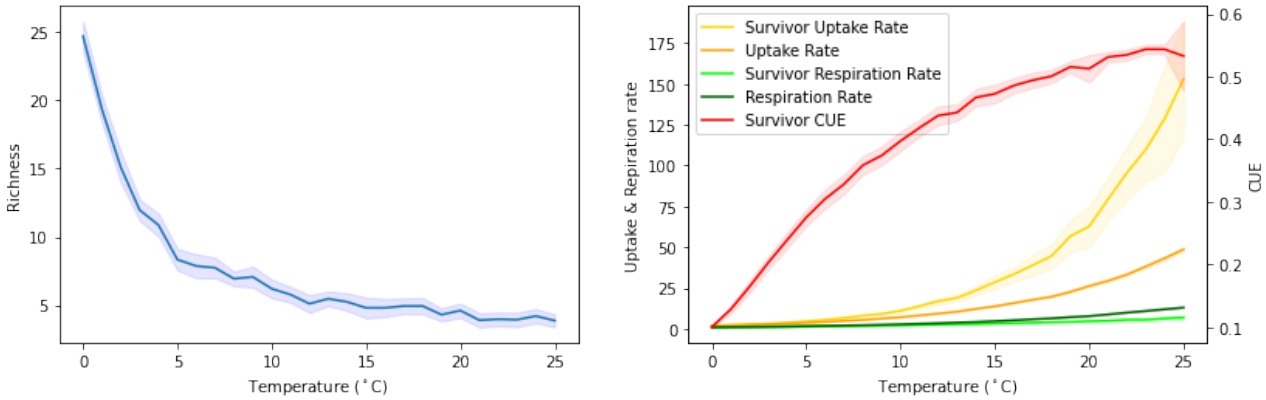

Figure 6: The left plot shows richness decreasing with increasing temperature inside operational temperature range; The right plot shows the selection of CUE values at different temperatures. As temperature increases, the uptake and respiration rates increase rapidly for every species, however only species with lower resource requirement survive (higher uptake rate and lower respiration rate), equivalent to the selection of higher CUE values.

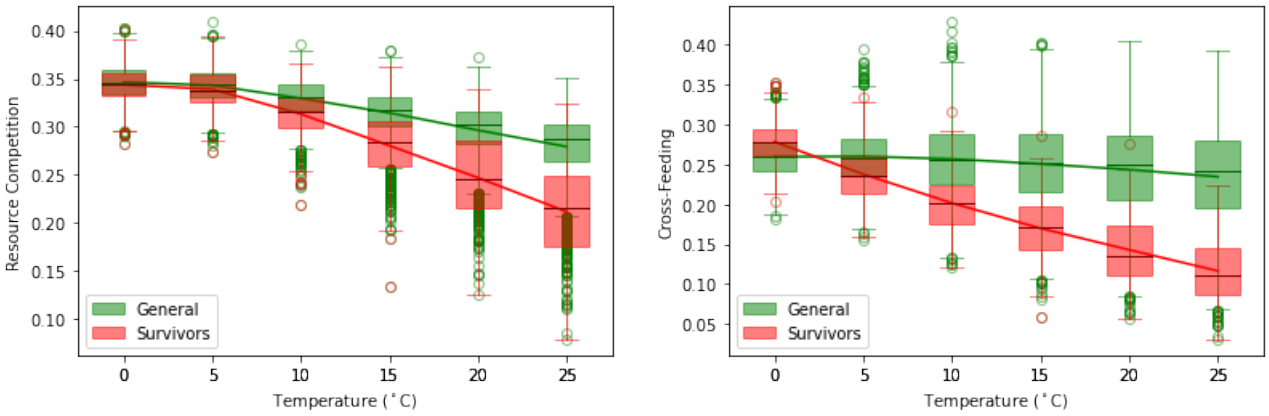

Figure 7: Higher temperature selects for less competition and less cooperation.

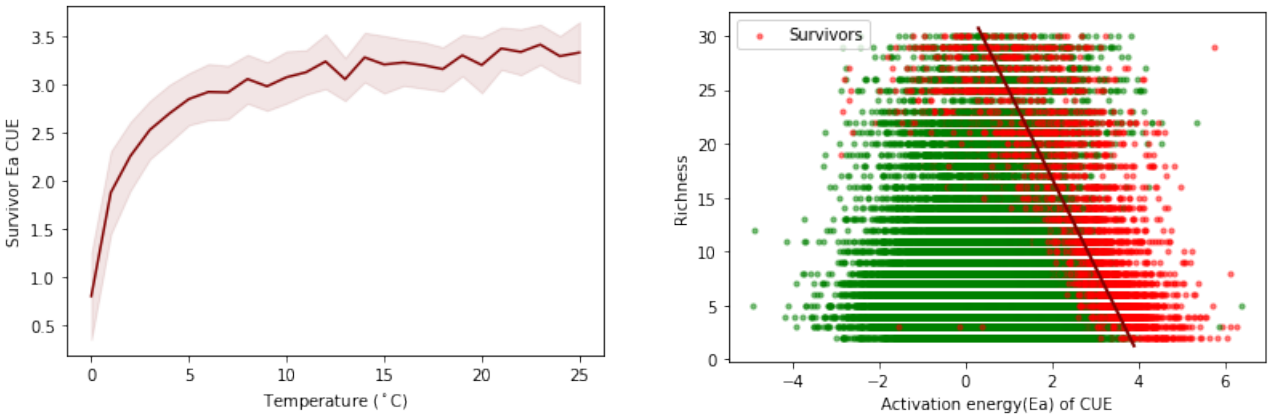

Figure 8: Temperature selection of the activation energy (Ea) for species CUE (upper), and the relation of Ea CUE with species richness (lower). Higher temperature environments favor specialists with higher Ea CUE values, and the stronger selection for higher Ea CUE values resulted in lower richness of the microbial community.

5 Discussion

One species one resource: 1/R

Severeal species one resource: The R* rule (Tilman 1982)

When the system reaches equilibrium, both dS/dt and $dC/dt = 0$. The resource concentration required for one species to survive (Sr_i) can be calculated as:

$$Sr_i = \frac{R_i}{\sum_{j=1}^{M} U_{ij}(1 - l_j)} \tag{12}$$

$$CUE_i = (1 - Sr_i)(1 - \sum_{j=1}^{M} l_j) \tag{13}$$

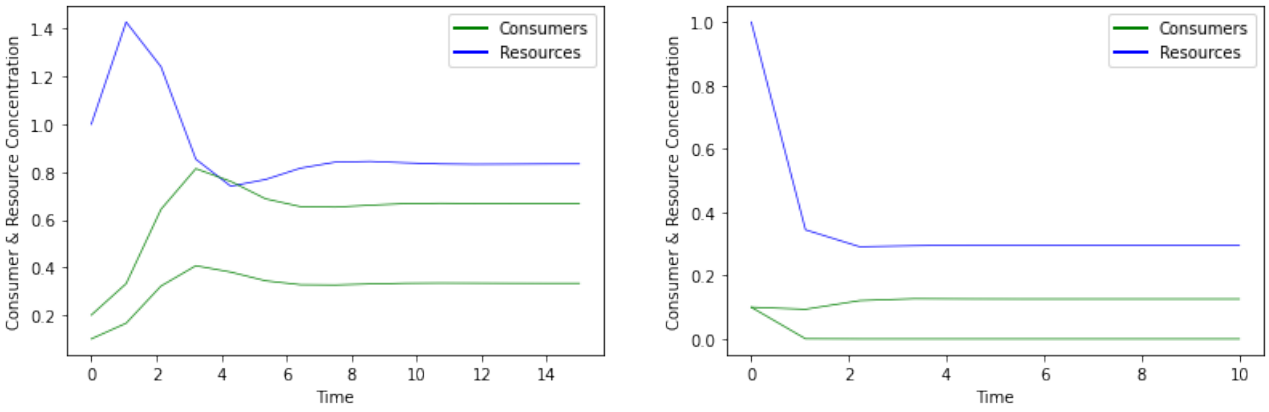

Figure 9: Example plot of the consumers and resource concentration dynamics of two species competing for one resource at reference temperature (left) and at 25 °C (right).

References

Bardgett, R. D., Freeman, C. & Ostle, N. J. (2008), 'Microbial contributions to climate change through carbon cycle feedbacks', *The ISME journal* **2**(8), 805–814.

Chase, J. M. & Myers, J. A. (2011), 'Disentangling the importance of ecological niches from stochastic processes across scales', *Philosophical transactions of the Royal Society B: Biological sciences* **366**(1576), 2351–2363.

Chesson, P. (2000), 'Mechanisms of maintenance of species diversity', *Annual review of Ecology and Systematics* **31**(1), 343–366.

Davidson, E. A. & Janssens, I. A. (2006), 'Temperature sensitivity of soil carbon decomposition and feedbacks to climate change', *Nature* **440**(7081), 165–173.

Domeignoz-Horta, L. A., Pold, G., Liu, X.-J. A., Frey, S. D., Melillo, J. M. & DeAngelis, K. M. (2020), 'Microbial diversity drives carbon use efficiency in a model soil', *Nature communications* **11**(1), 1–10.

Gang, F. (2019), 'A meta-analysis of the effects of warming and elevated co2 on soil microbes', *Journal of Resources and Ecology* **10**(1), 69–76.

Goldford, J. E., Lu, N., Bajić, D., Estrela, S., Tikhonov, M., Sanchez-Gorostiaga, A., Segrè, D., Mehta, P. & Sanchez, A. (2018), 'Emergent simplicity in microbial community assembly', *Science* **361**(6401), 469–474.

Goyal, A., Dubinkina, V. & Maslov, S. (2018), 'Multiple stable states in microbial communities explained by the stable marriage problem', *The ISME journal* **12**(12), 2823–2834.

Hendershot, J. N., Read, Q. D., Henning, J. A., Sanders, N. J. & Classen, A. T. (2017), 'Consistently inconsistent drivers of microbial diversity and abundance at macroecological scales'.

Kirk, J. L., Beaudette, L. A., Hart, M., Moutoglis, P., Klironomos, J. N., Lee, H. & Trevors, J. T. (2004), 'Methods of studying soil microbial diversity', *Journal of microbiological methods* **58**(2), 169–188.

Kolton, M., Marks, A., Wilson, R. M., Chanton, J. P. & Kostka, J. E. (2019), 'Impact of warming on greenhouse gas production and microbial diversity in anoxic peat from a sphagnum-dominated bog (grand rapids, minnesota, united states)', *Frontiers in microbiology* **10**, 870.

Kontopoulos, D.-G., Van Sebille, E., Lange, M., Yvon-Durocher, G., Barraclough, T. G. & Pawar, S. (2020), 'Phytoplankton thermal responses adapt in the absence of hard thermodynamic constraints', *Evolution* **74**(4), 775–790.

MacArthur, R. (1970), 'Species packing and competitive equilibrium for many species', *Theoretical population biology* **1**(1), 1–11.

Manzoni, S., Taylor, P., Richter, A., Porporato, A. & Ågren, G. I. (2012), 'Environmental and stoichiometric controls on microbial carbon-use efficiency in soils', *New Phytologist* **196**(1), 79–91.

Marsland III, R., Cui, W., Goldford, J., Sanchez, A., Korolev, K. & Mehta, P. (2019), 'Available energy fluxes drive a transition in the diversity, stability, and functional structure of microbial communities', *PLoS computational biology* **15**(2), e1006793.

Posfai, A., Taillefumier, T. & Wingreen, N. S. (2017), 'Metabolic trade-offs promote diversity in a model ecosystem', *Physical review letters* **118**(2), 028103.

Smith, T. P., Clegg, T., Bell, T. & Pawar, S. (2020), 'Systematic variation in the temperature dependence of bacterial carbon use efficiency', *bioRxiv* .

Smith, T. P., Thomas, T. J., García-Carreras, B., Sal, S., Yvon-Durocher, G., Bell, T. & Pawar, S. (2019), 'Community-level respiration of prokaryotic microbes may rise with global warming', *Nature communications* **10**(1), 1–11.

Theron, J. & Cloete, T. (2000), 'Molecular techniques for determining microbial diversity and community structure in natural environments', *Critical reviews in microbiology* **26**(1), 37–57.

Thompson, L. R., Sanders, J. G., McDonald, D., Amir, A., Ladau, J., Locey, K. J., Prill, R. J., Tripathi, A., Gibbons, S. M., Ackermann, G. et al. (2017), 'A communal catalogue reveals earth's multiscale microbial diversity', *Nature* **551**(7681), 457–463.

Tiedje, J. M., Asuming-Brempong, S., Nüsslein, K., Marsh, T. L. & Flynn, S. J. (1999), 'Opening the black box of soil microbial diversity', *Applied soil ecology* **13**(2), 109–122.

Tilman, D. (1982), *Resource Competition and Community Structure*, Princeton university press.

Tilman, D. (2004), 'Niche tradeoffs, neutrality, and community structure: a stochastic theory of resource competition, invasion, and community assembly', *Proceedings of the National Academy of Sciences* **101**(30), 10854–10861.

Vellend, M. (2010), 'Conceptual synthesis in community ecology', *The Quarterly review of biology* **85**(2), 183–206.

Zhou, J., Deng, Y., Shen, L., Wen, C., Yan, Q., Ning, D., Qin, Y., Xue, K., Wu, L., He, Z. et al. (2016), 'Temperature mediates continental-scale diversity of microbes in forest soils', *Nature communications* **7**(1), 1–10.

Zhou, Z., Wang, C. & Luo, Y. (2020), 'Meta-analysis of the impacts of global change factors on soil microbial diversity and functionality', *Nature communications* **11**(1), 1–10.